Title

Prediction equations for significant duration of earthquake ground motions considering site and near-source effects

Journal

Earthquake Spectra, 22(4)

ISSN

8755-2930

Authors

Kempton, Justin J
Stewart, Jonathan P

Publication Date

2006-11-01

Peer reviewed

Prediction Equations for Significant Duration of Earthquake Ground Motions Considering Site and Near-Source Effects

Justin J. Kempton[a] **and Jonathan P. Stewart,**[b] **M.EERI**

For engineering systems having a potential for degradation under cyclic loading (e.g., landslides, soil profiles subject to liquefaction, some structural systems), the characterization of seismic demand should include the amplitude and duration of strong shaking within the system. This article is concerned with significant-duration parameters, which are defined as the time interval across which a specified amount of energy is dissipated (as measured by the integral of the square of the ground acceleration or velocity). We develop ground-motion prediction equations for significant-duration parameters as a function of magnitude, closest site-source distance, site parameters that reflect shallow geologic conditions as well as deep basin structure, and near-source parameters. The relations are developed using a modern database and a random-effects regression procedure. We find significant duration to increase with magnitude and site-source distance (effects that had been identified previously), but also to decrease with increasing shear-wave velocity of near-surface sediments and to increase with increasing basin depth. Parameters that principally measure the duration of body waves were also found to decrease in near-fault areas subject to forward rupture directivity, although such effects were not apparent for other duration parameters that tend to reflect the combined duration of body and surface waves. [DOI: 10.1193/1.2358175]

INTRODUCTION

For structural or geotechnical systems whose performance is measured by damage that accumulates during shaking, duration has been shown to be a meaningful predictor of performance, along with amplitude and frequency content parameters. Example applications of duration for seismic performance characterization include the following:

- Seismic displacements of landslide masses have been related to the spatially averaged peak amplitude of shaking within the slide mass as well as the duration of shaking (e.g., Bray and Rathje 1998). Slope displacements were found to increase with duration.
- Pore pressure generation in liquefiable soils (e.g., Seed and Lee 1966) and volumetric strain accumulation in unsaturated soils (e.g., Silver and Seed 1971) both

[a] Senior Engineer, Kleinfelder, Inc., 1370 Valley Vista Drive, Suite 150, Diamond Bar, CA 91765
[b] Associate Professor and Vice Chair, Civil and Environmental Engineering Dept., University of California, Los Angeles, CA 90095-1593

Earthquake Spectra, Volume 22, No. 4, pages 985–1013, November 2006;

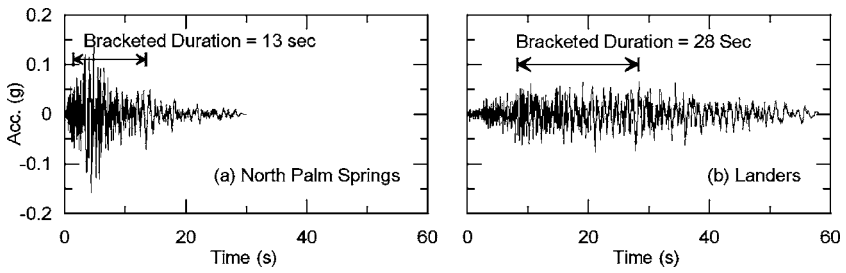

Figure 1. Evaluation of bracketed duration (acceleration threshold=0.05 g) for ground motions recorded at the North Palm Springs Airport site during M=6.0 and 7.3 earthquakes.

increase with the amplitude of shaking experienced by a soil element and with the number of cycles of shaking, N, at that amplitude. The N parameter, in turn, is correlated to the duration of shaking, although the degree of correlation depends on the specific duration definition and the method for counting cycles (Hancock and Bommer 2005, Bommer et al. 2006).

- Lateral spread displacements resulting from soil liquefaction have been related to amplitude and duration parameters of earthquake ground motions (Rauch and Martin 2000), with displacements found to increase with duration.
- Many types of structural components and systems can be subject to cyclic degradation, and hence would be expected to exhibit sensitivity to duration. Nonetheless, whether duration is a statistically significant predictor of structural damage remains an open question, with some research indicating no effect (Cornell 1997, Shome et al. 1998, Iervolino et al. 2006) and other research indicating a possible correlation (Reinoso et al. 2000, Hancock and Bommer 2004, Bommer et al. 2004). In support of the latter argument, inelastic response spectra (and its reduction from elastic spectra) have been correlated with duration by Chai et al. (1998) and Tiwari and Gupta (2000).

As described by Bommer and Martinez-Pereira (1999) and the references contained therein, many types of duration parameters have been proposed in the literature, but the most commonly used duration parameters are bracketed duration and significant duration. Example calculations of these parameters are shown in Figures 1 and 2. Figure 1 illustrates bracketed duration, which is defined as the time elapsed between the first and last excursions beyond a specified threshold acceleration (typically 0.05 g or 0.1 g). Bracketed duration parameters can be sensitive to the threshold accelerations and to small subevents occurring towards the end of a recording. For these and other reasons, other definitions of duration are often preferred.

Significant-duration parameters are defined as the time interval across which a specified amount of energy is dissipated. In this context, energy is represented by the integral of the square of the ground acceleration or velocity. The integral of ground acceleration is related to the Arias intensity (I_A) (Arias 1970), which is defined using the integral,

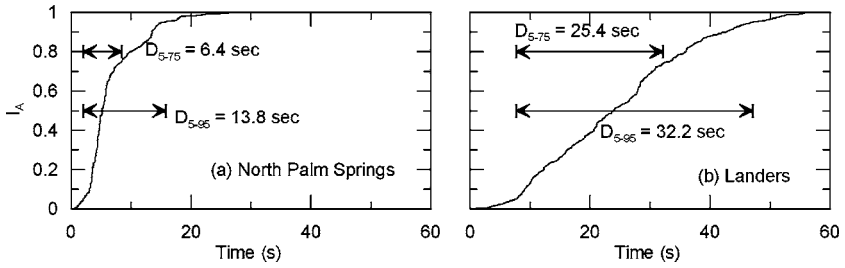

Figure 2. Evaluation of significant-duration parameters $D_{a5\text{-}75}$ and $D_{a5\text{-}95}$ for ground motions recorded at the North Palm Springs Airport site.

$$I_A = \frac{\pi}{2g}\int_0^T a^2(t)dt \tag{1}$$

where $a(t)$ is the acceleration time history, g is the acceleration of gravity, and T represents the complete duration of recording $a(t)$. Husid plots, used to track the build up of energy in time (Husid 1969), are shown in Figure 2. Two common measures of significant duration are time intervals between 5-75% and 5-95% of I_A (denoted as $D_{a5\text{-}75}$ and $D_{a5\text{-}95}$, respectively), which are indicated in Figure 2. The integral of ground velocity, introduced by Sarma (1970) and referred to as the energy integral by Anderson (2004), can also be used to define duration:

$$I_E = \int_0^\infty v^2(t)dt \tag{2}$$

where $v(t)$ is the velocity time history. Significant-duration parameters evaluated from the energy integral are denoted as $D_{v5\text{-}75}$ and $D_{v5\text{-}95}$.

The focus of the present work is on significant duration measured from the Arias and energy integrals. We select significant duration because it is relatively stable with respect to the definitions of beginning and end thresholds (Bommer and Martinez-Pereira 1999). Moreover, significant duration from the Arias integral has arguably seen the most use in recent engineering practice. It is recognized that nonzero significant durations can be measured for low amplitude records that are of little engineering significance; however, this problem is overcome when amplitude is coupled with duration for damage assessment, as is usually the case.

Ground motion prediction equations have been developed previously for bracketed duration, significant duration, and other duration parameters. All existing relationships include magnitude as a predictive parameter; some also consider site-source distance and site condition. Previous relations for significant duration are summarized in Table 1. Most previous relations were developed for $D_{a5\text{-}95}$. Table 1 indicates that the available prediction equations use different magnitude and distance definitions from one another and that site condition has most often been parameterized as rock or soil.

Table 1. Papers presenting prediction equations for significant duration defined from broadband accelerograms

Author	Duration Parameter[1]	Magnitude Type[2]	Distance Type[3]	Site Parameter[4]
Trifunac and Brady 1975	$D_{a5\text{-}95}$, $D_{v5\text{-}95}$, and $D_{d5\text{-}95}$	n/a	r_{epi}, h	soft alluvium, intermediate rock, and hard rock
Dobry et al. 1978	$D_{a5\text{-}95}$	n/a	n/a	rock
McGuire and Barnhard 1979	D_B, D_F, $D_{a5\text{-}95}$	n/a	r or r_{epi}	soil, rock
Kamiyama 1984	$D_{a5\text{-}95}$	M_J	r_{epi}, h	$f(V_S, d_i)$
Abrahamson and Silva 1996	$D_{a5\text{-}75}$ and $D_{a5\text{-}95}$	M	r	soil, rock

[1] Duration Parameters:
D_B=bracketed duration
D_F=fractional duration (time interval over which Arias intensity is uniformly distributed at an average power [Vanmarcke and Lai 1980])
$D_{a5\text{-}95}$=significant duration as function of the acceleration record
$D_{v5\text{-}95}$=significant duration as function of the velocity record
$D_{d5\text{-}95}$=significant duration as function of the displacement record
[2] Magnitude Parameters:
M_J=Japan Meteorological Agency magnitude
M=moment magnitude
[3] Distance Parameters:
r=site to source distance
r_{epi}=epicentral distance
h=hypocentral depth
[4] Site parameters:
V_S=shear-wave velocity
d_i=layer thicknesses

We note that a number of additional prediction equations (not shown in Table 1) have been developed for frequency-dependent duration parameters evaluated from band-passed accelerograms (e.g., Bolt 1973, Trifunac and Westermo 1977, Mohraz and Peng 1989, Novikova and Trifunac 1994). Novikova and Trifunac (1994) argue that an advantage of modeling duration using frequency bands is that the arrival time and duration of each separate strong-motion pulse can be evaluated, which can provide insight into source effects and energy dissipation between strong-motion pulses. However, engineering applications of duration consistently use duration parameters derived from full broadband records. This practice is followed here because seismic excitation of structures is broadband, and intensity measures should characterize that broadband excitation (an analogous situation is the use of spectral acceleration, defined from broadband accelerograms, to characterize the amplitude of shaking in structures). Accordingly, we focus on duration parameters for broadband accelerograms.

There are several shortcomings to the existing ground-motion prediction equations for significant duration, which we seek to address in the present study:

1. Most existing relations utilize a functional form that lacks a physically based representation of magnitude effects on source duration.
2. The distance measure used previously has typically been epicentral distance, not closest site-source distance (accounting for the source dimension).
3. Relations derived from the energy integral are not available; such relations are of interest because they would be expected to capture the duration of long-period components of ground motions more effectively than duration parameters derived from accelerograms.
4. The effects of site condition on duration have not been satisfactorily investigated.
5. The only existing model for near-fault rupture directivity effects on duration (Somerville et al. 1997) utilizes a database that is now dated, especially in light of significant new data inventories compiled as part of the PEER Next Generation Attenuation (NGA) project (http://peer.berkeley.edu/nga/).
6. Existing relationships were derived using least-squares regression. This method of analysis gives equal weight to each recording, and hence does not properly account for correlations among the data recorded during a given event (which might cause the durations for a particular earthquake to be unusually large or small).

The objective of the work described in this article is to develop prediction equations for significant duration that (1) rationally account for the effects of magnitude, distance, site condition, and near-fault rupture directivity; and (2) are based on a mixed-effects regression procedure that accounts for inter- and intra-event ground-motion variability.

STRONG-MOTION DATABASE

We used a ground-motion database consisting of 1,829 recordings from 149 earthquakes. These recordings are based on worldwide shallow crustal earthquakes near active plate margins. Subduction and intra-plate events are excluded. Due to recordings with unknown or poor estimates of magnitude, distance, or site condition, the data set was reduced to 1,559 recordings from 73 events. Table 2 lists the reduced data set, which provides a reasonable amount of data over a magnitude range of $M \approx 5-7.6$ and closest site-source distance range $r \approx 0-200$ km. Figure 3 shows the M and r distribution represented in the database. Magnitude (M) is taken as moment magnitude where available, and is otherwise taken as surface wave magnitude for $M > 6$ and local magnitude for $M < 6$. The data were obtained from the strong-motion database maintained by the Pacific Earthquake Engineering Research Center (http://peer.berkeley.edu/smcat/). This data set has been uniformly processed, which is important to avoid artificial record-to-record variations in duration that might result from variable processing.

Included in the strong-motion database are near-fault rupture directivity parameters as defined by Somerville et al. (1997). Rupture directivity parameters were originally compiled by Somerville et al. (1997), and were recently updated by Somerville and co-

Table 2. Summary of strong-motion database used in this study

Event	Year	Mo-day	Time	Magnitude	Distance Range (km)	Number of Recordings
Imperial Valley	1940	519	437	7.0	8.3	1
Kern County	1952	721	1153	7.4	41–127	5
San Francisco	1957	322	1944	5.3	9.5	1
Parkfield	1966	628	426	6.1	0.1–60	5
Borrego Mtn	1968	409	230	6.8	46–217.4	5
Lytle Creek	1970	912	1430	5.4	15.4–107.8	10
San Fernando	1971	209	1400	6.6	2.8–223	55
Point Mugu	1973	221	1445	5.8	25	1
Hollister	1974	1128	2301	5.2	11.1–12.3	3
Oroville	1975	801	2020	6.0	9.5	1
Oroville	1975	802	2022	5.0	12.7–14.6	2
Oroville	1975	802	2059	4.4	11.1–15	3
Oroville	1975	808	700	4.7	6.5–13.3	9
Friuli, Italy	1976	506	2000	6.5	34.6–97.1	5
Gazli, USSR	1976	517		6.8	3	1
Friuli, Italy	1976	915	315	6.1	10.8–36.1	4
Santa Barbara	1978	813		6.0	14–36.6	2
Tabas, Iran	1978	916		7.4	3–199.1	7
Coyote Lake	1979	806	1705	5.7	3.1–31.2	10
Imperial Valley	1979	1015	2316	6.5	0.5–54.1	35
Imperial Valley	1979	1015	2319	5.2	12.2–52.1	16
Imperial Valley	1979	1016	658	5.5	11.2	1
Livermore	1980	124	1900	5.8	12.9–37.3	7
Livermore	1980	127	233	5.4	3.6–31	8
Anza (Horse Cany)	1980	225	1047	4.9	5.8–40.6	5
Mammoth Lakes	1980	527	1901	4.9	1.8–9.9	6
Mammoth Lakes	1980	531	1516	4.9	7.3–11.8	7
Victoria, Mexico	1980	609	328	6.4	34.8–62.6	5
Mammoth Lakes	1980	611	441	5.0	7.6–14.2	9
Taiwan SMART1(5)	1981	129		5.7	21	7
Westmorland	1981	426	1209	5.8	10.1–26.5	6
Coalinga	1983	502	2342	6.4	8.5–55.2	49
Coalinga	1983	509	249	5.0	12.1–20.3	21
Coalinga	1983	611	309	5.3	9.7–10.5	3
Coalinga	1983	709	740	5.2	10–17	11
Coalinga	1983	722	239	5.8	8.2–17.4	11
Coalinga	1983	722	343	4.9	12.1–13.7	2
Coalinga	1983	725	2231	5.2	12.7–14.7	2
Coalinga	1983	909	916	5.3	13.7–18.4	2
Morgan Hill	1984	424	2115	6.2	0.1–71.2	31
Bishop (Rnd Val)	1984	1123	1912	5.8	19	1
Nahanni, Canada	1985	1223		6.8	6–16	3

Table 2. (**cont.**)

Event	Year	Mo-day	Time	Magnitude	Distance Range (km)	Number of Recordings
Hollister	1986	126	1920	5.4	14.9–16.9	4
Taiwan SMART1(40)	1986	520		6.4	64	8
N. Palm Springs	1986	708	920	6.0	7.3–82.8	32
Chalfant Valley	1986	720	1429	5.9	11–27	5
Chalfant Valley	1986	721	1442	6.2	9.2–50.8	11
Chalfant Valley	1986	721	1451	5.6	14–20	3
Chalfant Valley	1986	731	722	5.8	13–21	2
Whittier Narrows	1987	1001	1442	6.0	9–105	121
Whittier Narrows	1987	1004	1059	5.3	12.6–42.7	11
Superstitn Hills(A)	1987	1124	514	6.3	24.7	1
Superstitn Hills(B)	1987	1124	1316	6.7	0.7–28.3	11
Spitak, Armenia	1988	1207		6.8	30	1
Loma Prieta	1989	1018	5	6.9	5.1–99.2	65
Big Bear	1992	628	805	6.4	8.6–151	39
Cape Mendocino	1992	425	1806	7.1	8.5–44.6	6
Landers	1992	628	1158	7.3	0–194.1	69
Northridge	1994	117	1231	6.7	2.6–146.5	159
Northridge Aftershock	1994	117	431	5.9	8.9–85	26
Northridge Aftershock	1994	117	440	5.2	11–46.3	8
Northridge Aftershock	1994	117	1533	5.6	19.9–58.5	9
Northridge Aftershock	1994	117	1643	5.2	22.6–61.8	8
Northridge Aftershock	1994	320	1320	5.2	13.4–92.2	29
Double Springs	1994	912	1223	6.1	17.7	1
Kobe, Japan	1995	116	2046	6.9	0.2–157.2	25
Kozani, Greece	1995	513	847	6.6	18.9–92.8	6
Dinar, Turkey	1995	1001	1557	6.2	26.3–243.3	5
Aqaba, Jordan	1995	1122	616	7.1	93.8	1
Izmit, Turkey	1999	817	0302	7.4	5–183.3	21
Chi-Chi, Taiwan	1999	921	0147	7.6	0.23–185.5	398
Duzce, Turkey	1999	1012	1657	7.2	0.9–188.4	21
Hector Mine	1999	1016	946	7.1	48.6–245	75

workers as part of the NGA project (Graves 2004, pers. comm.). Near-fault parameters from the NGA project were used in the present study. There are a total of 306 recordings from 27 events for which rupture directivity parameters are available.

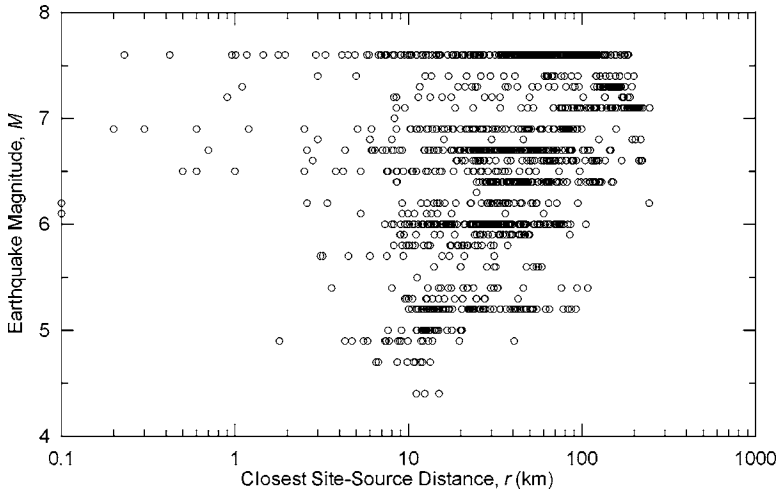

Figure 3. Distribution of strong-motion data used in this study.

Two types of site parameters were compiled for the strong-motion sites in the database. The first is intended to represent the properties of near-surface sediments. The parameter $V_{s\text{-}30}$ was used for this purpose, which is the ratio of 30 m to the vertical shear-wave travel time through the upper 30 m of the site. Parameter $V_{s\text{-}30}$ has been found to be an effective predictor of site effects on response spectral acceleration (e.g., Borcherdt 1994, Choi and Stewart 2005), and forms the basis of site classifications used in building codes (e.g., Dobry et al. 2000). A database of $V_{s\text{-}30}$ parameters was compiled for strong-motion sites by Stewart et al. (2001) and has been continuously updated over time as additional data has become available (Stewart et al. 2005). The database used here matches that of Stewart et al. (2005). The database includes sites where $V_{s\text{-}30}$ values were measured based on boreholes near the station, as well as sites where $V_{s\text{-}30}$ values were estimated as part of the NGA project. Velocity estimates were based on classified surface geology by Borcherdt and coworkers (e.g., Borcherdt and Glassmoyer 1994, Borcherdt 2002), geologic classifications by Christopher Wills (developed as part of the NGA project), or Geomatrix site classifications by Walter Silva. Figure 4 presents a histogram of $V_{s\text{-}30}$ values for the strong ground-motion sites used in this study. There are a total of 557 sites for which $V_{s\text{-}30}$ values are available. Those sites have produced 968 recordings from 48 events.

The second type of site parameter is intended to represent the effects of relatively deep basin structure. The parameterization of basin effects involves the use of a depth term and an index to differentiate sites located in basins overlying the seismic source from those in basins located to the side of the seismic source. Depth is parameterized by distance from the ground surface to the 1.5 km/s shear-wave isosurface, which is denoted $z_{1.5}$. Depth terms are evaluated for sites in southern California and the San Francisco Bay Area using the basin models of Magistrale et al. (2000) and Hole et al. (2000), respectively. The index related to source/basin location is defined as follows:

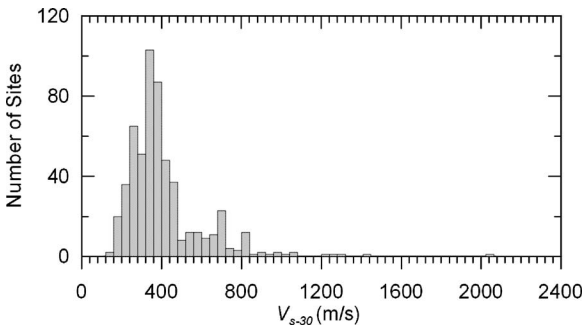

Figure 4. Histogram of $V_{s\text{-}30}$ values for sites used in this study (measured+estimated velocities).

- Coincident source and site basin locations (CBL)
- Distinct source and site basin locations (DBL)

Detailed protocols for establishment of the CBL and DBL conditions for a given site/earthquake pair are given in Choi et al. (2005). There are 563 recordings from 22 events for which basin depth parameters are available; a subset consisting of 284 recordings also has DBL/CBL designations.

REGRESSION MODEL

The form of the regression model described here is similar to that used previously by Abrahamson and Silva (1996). Theoretical seismic source models formulated in the frequency domain (e.g., Hanks and McGuire 1981, Boore 1983) suggest that source duration (D_{source}) is inversely related to a corner frequency f_c in the Fourier amplitude spectrum (when Fourier amplitude spectra are plotted in log-log space, f_c denotes the frequency that separates a relatively flat portion of the spectrum at mid-frequencies from a decaying region at low frequencies).

$$D_{source} = \frac{1}{f_c} \tag{3}$$

Brune (1970, 1971) has related f_c to the seismic moment and stress drop as follows:

$$f_c = 4.9 \cdot 10^6 \beta (\Delta\sigma / M_0)^{1/3} \tag{4}$$

where β is the shear-wave velocity at the source (taken as 3.2 km/s), $\Delta\sigma$ is the stress drop (in bars), and M_0 is the seismic moment (in dyne-cm). We refer to $\Delta\sigma$ as "stress drop index" in lieu of "stress drop" to emphasize that it is not the true stress drop of the earthquake event (Atkinson and Beresnev 1997), but simply an estimate of stress drop based on analysis of duration parameters within the context of the Brune source model.

Increases in significant duration associated with wave propagation and site effects are taken as additive to the source term, i.e.,

$$SD = \frac{1}{f_c(M_0, \Delta\sigma)} + f_1(r) + f_2(S) \tag{5}$$

where SD represents significant duration, $f_1(r)$ represents the distance dependence. and $f_2(S)$ represents the site dependence. The rationale for the additive (as opposed to multiplicative) distance term is that the spreading of seismic waves with distance would be expected to be similar for small- and large-magnitude earthquakes since the wave propagation velocities are similar. Likewise, extensions of duration due to site effects such as resonance within sedimentary layers or basin trapping would be expected to extend durations a fixed amount of time (which would be a function of the sediment stratigraphy and seismic velocities), regardless of the duration of shaking on the reference (rock) condition.

The spreading in time of seismic waves with distance from the source is related to their propagation velocities. Accordingly, the distance dependence is taken as linear:

$$f_1(r) = c_2 r \tag{6}$$

where c_2 is a regression parameter. The site dependence of significant duration is evaluated in several ways, and is addressed subsequently. Therefore, the base model for the regression analysis is written as follows:

$$\ln(SD)_{ij} = \ln\left[\frac{\left(\frac{\Delta\sigma}{10^{1.5M_i+16.05}} \right)^{-1/3}}{4.9 \cdot 10^6 \beta} + c_2 r_{ij} + f_2(S_{ij}) \right] + \eta_i + \varepsilon_{ij} \tag{7}$$

where η_i is the event term for earthquake event i (explained below) and ε_{ij} represents the residual for recording j in event i. In Equation 7, seismic moment is converted to magnitude (M) as $M_0 = 10^{1.5M+16.05}$ (Hanks and Kanamori 1979). The natural logarithm of significant duration is used because duration is assumed to be lognormally distributed (details given below). By using the natural log of the significant duration, ε_{ij} is normally distributed.

Regression analyses utilizing Equation 7 are performed using mixed-effects procedures similar to Abrahamson and Youngs (1992) as implemented in the program R (Pinheiro and Bates 2000). Mixed-effects regression is a maximum-likelihood method that accounts for correlations in the data recorded by a single earthquake (i.e., the data for a given event may have unusually low or high durations, as represented by event term η_i). Mixed-effects regressions produce two types of error terms: inter-event terms and intra-event terms. The total standard deviation σ_{total} of the data combines the inter- and intra-event variability,

Table 3. Regression parameters for preliminary models with stress drop index independent of magnitude

	$\Delta\sigma$ (bars)	c_1	c_2	β	τ	σ	σ_{total}
$D_{a5\text{-}75}$	411±164	0.52±0.23	0.07±0.01	3.2	0.37	0.44	0.57
$D_{a5\text{-}95}$	24±9	1.91±0.50	0.15±0.02	3.2	0.34	0.38	0.51
$D_{v5\text{-}75}$	236±114	1.17±0.38	0.10±0.02	3.2	0.44	0.52	0.68
$D_{v5\text{-}95}$	7.7±3.2	2.47±0.42	0.15±0.03	3.2	0.47	0.39	0.61

$$\sigma_{total} = \sqrt{\sigma^2 + \tau^2} \tag{8}$$

where σ=intra-event standard deviation (i.e., standard deviation of ε_{ij}) and τ=inter-event standard deviation (i.e., standard deviation of η_i).

REGRESSION RESULTS

PRELIMINARY MODEL FOR EVALUATION OF SOURCE AND PATH EFFECTS

We begin by using a simple binary site model in which site condition is parameterized as $S=0$ for rock and $S=1$ for soil. This is done to minimize the number of regression parameters, which optimizes the estimation of source and path parameters. With the simple binary site parameter, site term $f_2(S)$ has only one regression coefficient:

$$f_2 = c_1 S \tag{9}$$

where c_1 is the regression coefficient. Regression analyses are performed according to Equation 7 with the above substitution for the site term.

We begin by taking $\Delta\sigma$ as a constant, and hence simultaneously regress on parameters c_1, c_2, and $\Delta\sigma$. The results for each of the four duration parameters ($D_{a5\text{-}75}, D_{a5\text{-}95}, D_{v5\text{-}75}, D_{v5\text{-}95}$) are listed in Table 3. The estimation errors in Table 3 are the half-widths of the ±95% confidence intervals. Figure 5a shows an example histogram of the intra-event model residuals. The natural logs of the intra-event residuals for

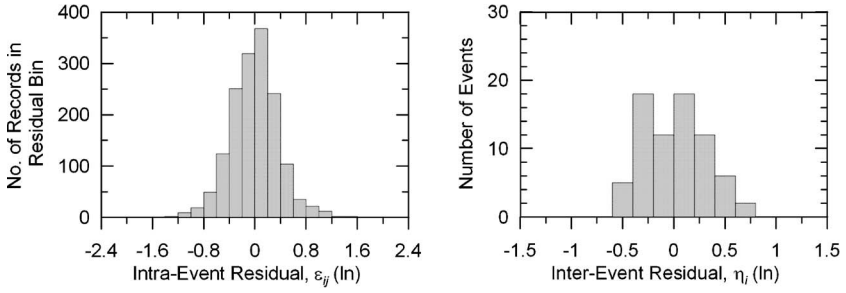

Figure 5. Histogram of residuals for significant-duration parameter $D_{a5\text{-}95}$.

Table 4. Stress drop index ($\Delta\sigma$) for discrete magnitude bins

Magnitude bin	$D_{a5\text{-}75}$	$D_{a5\text{-}95}$	$D_{v5\text{-}75}$	$D_{v5\text{-}95}$
4.4 to 5.0	211±385	2.7±4.0	37±120	0.3±0.5
5.0 to 5.5	1079±2493	7.5±7.9	1652±5950	1.2±1.1
5.5 to 6.0	287±316	6.6±5.6	52±70	1.8±1.9
6.0 to 6.5	725±752	33±22	238±250	9.3±6.3
6.5 to 7.0	513±318	61±33	357±258	30±16
7.0 to 7.5	524±299	93±42	183±155	45±31
7.6 (Chi-Chi)	334±128	12±15	147±142	5.2±6.9

$D_{a5\text{-}75}$ are found to be normally distributed per the chi-square test (Ang and Tang 1975, p. 274) at a significance level of 95%; the other duration parameters are not normally distributed at the 95% significance level (e.g., $D_{a5\text{-}75}$ in Figure 5b), although the normal distribution provides a better fit than other distributions considered such as lognormal. Figure 5b similarly shows a histogram of inter-event residuals (event terms), which were generally found to be normally distributed at a significance level of 95%. Based on these results, we assume a lognormal distribution for the duration data.

No significant variations in bias were found when the data is grouped by rupture mechanism (reverse, normal, strike-slip). Accordingly, this effect is not considered subsequently. We note that bilateral fault ruptures (such as from the 1989 Loma Prieta, California, earthquake) have been shown to produce reduced durations relative to unilateral ruptures (Bommer and Martinez-Pereira 1999). However, this effect is not considered since the occurrence of bilateral rupture is not predictable, and hence event-to-event variability in bilateral versus unilateral rupture contributes to the inter-event standard deviation τ.

As shown in Table 3, the stress drop index, $\Delta\sigma$, varies significantly between the 5-75 duration parameters (for which it is relatively large) and the 5-95 duration parameters (for which it is small). This is a consequence of 5-95 durations being significantly larger than 5-75 durations (e.g., Figure 2), which forces a lower $\Delta\sigma$ term per the selected functional form in Equation 7. These differences highlight that fact that $\Delta\sigma$ is a stress drop *index* related to the duration definition and the functional form of the regression model, and is not a true stress drop.

We expect that the stress drop index $\Delta\sigma$ may be magnitude dependent based on physical considerations (increased fault slip in large-magnitude earthquakes should cause increased stress drop) and previous experience with similar models [magnitude-dependent stress drop terms were identified for duration by Abrahamson and Silva (1996) and for equivalent number of cycles by Liu et al. (2001)]. To investigate the magnitude dependence of $\Delta\sigma$, we sort the data into magnitude bins (i.e., M =4.4–5.0, 5.0–5.5, etc.), then perform regression analyses according to Equation 7 (with site term from Equation 9) with c_1 and c_2 fixed at the values in Table 3. Hence $\Delta\sigma$ is the only free parameter. The results are presented in Table 4, and are plotted for the $D_{a5\text{-}75}$ and $D_{a5\text{-}95}$ parameters in Figures 6 and 7.

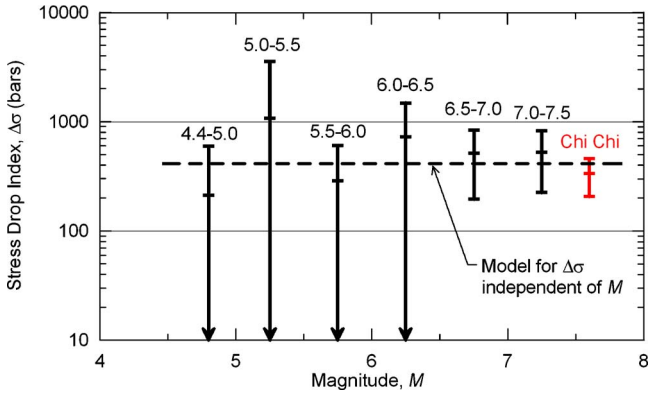

Figure 6. Estimated stress drop index and model for stress drop independent of magnitude for the $D_{a5\text{-}75}$ data.

For parameters $D_{a5\text{-}75}$ and $D_{v5\text{-}75}$, the stress drop has no clear magnitude dependence, so a constant $\Delta\sigma$, set at the values from Table 3, is adequate (the horizontal line in Figure 6 is drawn at this value of $\Delta\sigma$). For parameters $D_{a5\text{-}95}$ and $D_{v5\text{-}95}$, $\Delta\sigma$ increases with magnitude (e.g., Figure 7). To capture the trend of magnitude-dependent stress drop, an exponential model for $\Delta\sigma$ was adopted:

$$\Delta\sigma = \exp[b_1 + b_2(M - M^*)] \tag{10}$$

where b_1 and b_2 are regression coefficients and M^* is a reference magnitude taken as 6.

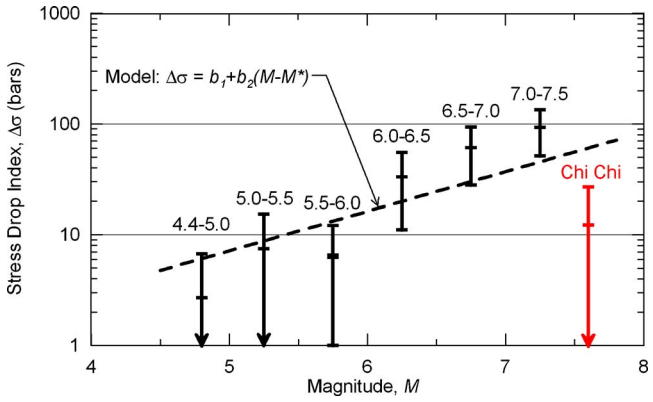

Figure 7. Estimated stress drop index and model for stress drop as a function of magnitude for the $D_{a5\text{-}95}$ data.

Table 5. Regression coefficients for magnitude-dependent stress drop index ($\Delta\sigma$)

	b_1	b_2	$1-p^1$	c_1^*	c_2^*	β^*	τ	σ	σ_{total}
D_{a5-75}	6.02±0.40	n/a	n/a	0.52	0.07	3.2	0.37	0.44	0.57
D_{a5-95}	2.79±0.36	0.82±0.38	1.00	1.91	0.15	3.2	0.27	0.38	0.47
D_{v5-75}	5.46±0.48	n/a	n/a	1.17	0.10	3.2	0.44	0.50	0.66
D_{v5-95}	1.53±0.37	1.34±0.40	1.00	2.47	0.15	3.2	0.34	0.40	0.52

[1] rejection confidence for a $b_2=0$ model (null hypothesis of zero slope)
[*] Identical to values in Table 3

When Equation 10 is used to represent the stress drop index, the regression equation becomes

$$\ln(SD)_{ij} = \ln\left[\frac{\left(\frac{\exp(b_1 + b_2(M_i - M^*))}{10^{1.5M_i+16.05}}\right)^{-1/3}}{4.9\cdot 10^6\beta} + c_2 r_{ij} + f_2(S)_{ij}\right] + \eta_i + \varepsilon_{ij} \qquad (11)$$

Parameters b_1 and b_2 were estimated by performing regression analyses with Equation 11 (site term from Equation 9) with c_1 and c_2 fixed at the values in Table 3. The results are listed in Table 5, and the resulting models for stress drop index are plotted as lines in Figures 6 and 7.

As shown in Figures 6 and 7, the Chi Chi earthquake data shows significantly lower stress drop index than the neighboring bin of $M=7.0-7.5$. This implies higher durations from Chi Chi than other earthquakes with similar (although slightly lower) magnitude. This low value of stress drop is consistent with unusually low high-frequency ground-motion amplitudes recorded during that earthquake (e.g., Boore 2001). Nonetheless, the Chi Chi event is now generally included in strong-motion databases for shallow crustal earthquakes in active tectonic regions (e.g., the data is included in the NGA database), and hence data from this event was included for the regression analyses of $\Delta\sigma$, b_1, and b_2.

To test the statistical significance of the magnitude dependence of stress drop for parameters D_{a5-95} and D_{v5-95}, we compile sample 't' statistics to test the null hypothesis that $b_2=0$. This statistical testing provides a significance level=p that the null hypothesis cannot be rejected. For clarity of expression, we tabulate in Table 5 values of 1-p, which we refer to as a "rejection confidence for a $b_2=0$ model." The large rejection confidence levels (i.e., >95%) shown in Table 5 indicate significant magnitude-dependence in stress drop index. This is further demonstrated by the b_2 values being greater than their standard error. Note also that by utilizing the magnitude-dependent stress drop, the standard deviation (σ_{total}) drops by 0.04 for D_{a5-95} and 0.09 for D_{v5-95} (seen by comparing Tables 3 and 5).

The model residuals (i.e., residual=data−model in natural logarithmic units) are plotted as functions of M and r in Figure 8 for parameter D_{a5-95}. The results show no

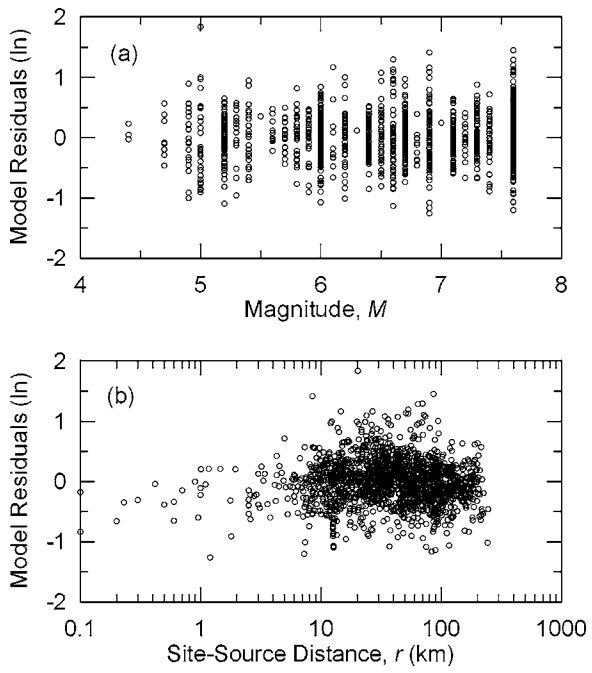

Figure 8. Residuals of regression model with magnitude-dependent stress drop for $D_{a5\text{-}95}$ plotted as function of magnitude (M) and distance (r).

clear bias with respect to magnitude, but a clear overprediction bias at small distances ($r < \sim 20$ km). Residuals for the other duration parameters show similar trends (Kempton 2004). This bias is addressed subsequently in this article.

BASE MODEL INCLUDING SHEAR-WAVE-VELOCITY-DEPENDENT SITE TERM

Figure 9a shows the residuals of the preliminary model developed above plotted against $V_{s\text{-}30}$. The linear trend line shows decreasing residual with increasing $V_{s\text{-}30}$ (i.e., increasing overprediction of duration with increasing $V_{s\text{-}30}$). Accordingly, a site term that linearly varies with $V_{s\text{-}30}$ is selected:

$$f_2 = c_4 + c_5(V_{s\text{-}30}) \tag{12}$$

Functional forms for f_2 that use the log of $V_{s\text{-}30}$ were also considered, but the linear $V_{s\text{-}30}$ term was found to produce a lower standard deviation of residuals. Incorporating the substitution in Equation 12, the regression equation (Equation 11) is expanded to

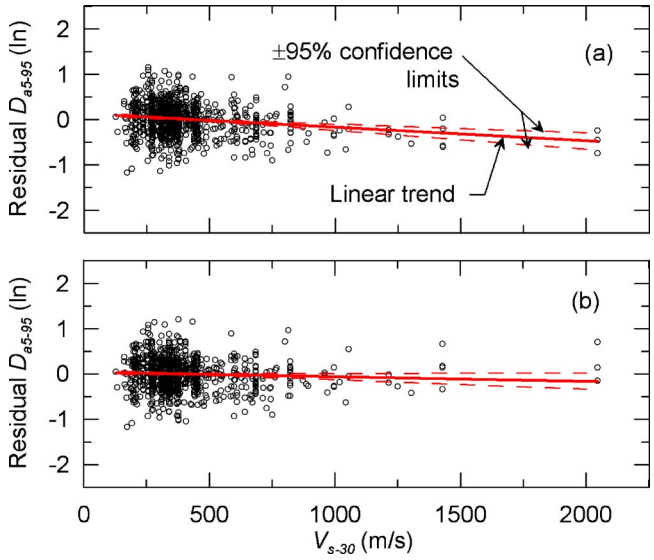

Figure 9. Residuals of regression model for $D_{a5\text{-}95}$ plotted as function of $V_{s\text{-}30}$ for (a) preliminary model (rock/soil site term) and (b) base model (velocity-dependent site term).

$$\ln(SD)_{ij} = \ln\left[\frac{\left(\frac{\exp(b_1 + b_2(M_i - M^*))}{10^{1.5M_i+16.05}}\right)^{-1/3}}{4.9 \cdot 10^6 \beta} + r_{ij}c_2 + (c_4 + c_5(V_{s\text{-}30})_{ij})\right] + \eta_i + \varepsilon_{ij} \tag{13}$$

Mixed-effects regression analyses were performed according to Equation 13, but with c_2, b_1, and b_2 fixed at the values in Table 5. The database utilized for these analyses is smaller than that utilized for the preliminary analyses, because not all strong-motion sites have $V_{s\text{-}30}$ values (968 recordings from 48 earthquakes in the present analyses versus 1,557 recordings from 73 earthquakes previously). These regression analyses are used only to establish regression coefficients c_4 and c_5 (other parameters are fixed at their previous values). The results are listed in Table 6. We define the "base model" for

Table 6. Regression coefficients for model that includes $V_{s\text{-}30}$-based site term

	c_4	c_5	$1-p^1$	b_1^*	b_2^*	c_2^*	β^*	τ	σ	σ_{total}
$D_{a5\text{-}75}$	0.82±0.34	−0.0013±0.0004	1.00	6.02	n/a	0.07	3.2	0.32	0.42	0.53
$D_{a5\text{-}95}$	3.00±0.82	−0.0041±0.0008	1.00	2.79	0.82	0.15	3.2	0.26	0.36	0.44
$D_{v5\text{-}75}$	1.40±0.58	−0.0022±0.0005	1.00	5.46	n/a	0.10	3.2	0.45	0.51	0.68
$D_{v5\text{-}95}$	3.99±1.29	−0.0062±0.0011	1.00	1.53	1.34	0.15	3.2	0.31	0.39	0.50

[1] rejection confidence for a c_5=0 model (null hypothesis of zero slope)
* Identical to values in Table 3

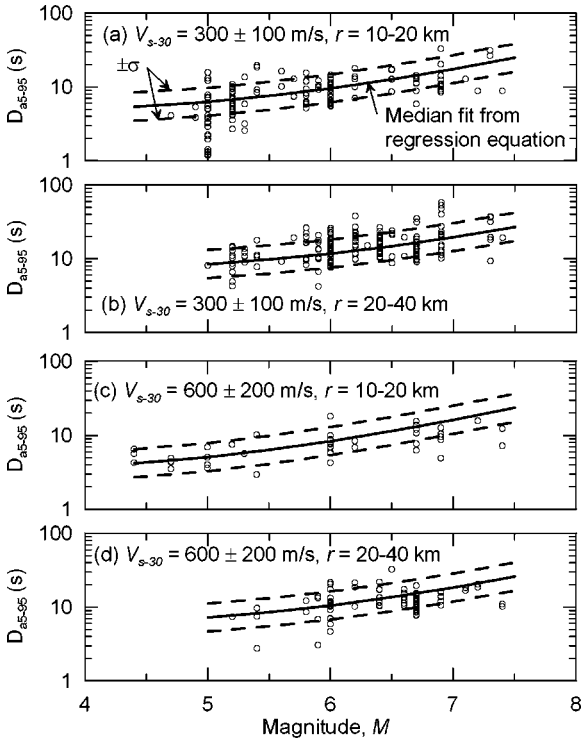

Figure 10. Plots of model vs. data for $D_{a5\text{-}95}$.

significant duration as Equation 13 coupled with the regression coefficients in Table 6.

The hypothesis test results listed in Table 6 indicate that the slope parameter (c_5) is statistically significant for each of the duration parameters. The standard-deviation terms (σ_{total}) are generally lower as a result of utilizing the $V_{s\text{-}30}$-dependent site term (comparing Tables 5 and 6). Residuals for $D_{a5\text{-}95}$ are plotted as a function of $V_{s\text{-}30}$ in Figure 9b along with linear fit lines. The previously noted trend (from Figure 9a) has been effectively removed by the $V_{s\text{-}30}$-dependent site term. Residuals against magnitude and distance are not significantly different from what was shown previously in Figure 8 (Kempton 2004).

The above results for parameters c_4 and c_5 can be used to estimate the reference site condition for the duration models, which is the condition for which $f_2(S)=0=-c_4/c_5$. This reference velocity is 630–640 m/s for $D_{a5\text{-}75}$, $D_{v5\text{-}75}$, and $D_{v5\text{-}95}$, and 730 m/s for $D_{a5\text{-}95}$.

In Figure 10, the model for $D_{a5\text{-}95}$ (±one standard deviation) is plotted through the data in the r=10–20 km and r=20–40 km distance ranges for sites with $V_{s\text{-}30}$ =200–400 m/s (model is plotted for $V_{s\text{-}30}$=300 m/s) and $V_{s\text{-}30}$=400–800 m/s (model

is plotted for $V_{s\text{-}30}$=600 m/s). The model predictions appear to be generally compatible with the data. Similar results are obtained for other duration parameters (Kempton 2004).

DEPENDENCE OF BASE MODEL RESIDUALS ON BASIN PARAMETERS

We evaluate the effects of deep basin structure on significant duration by adding a linear function of basin depth to the site term, i.e.,

$$f_2 = c_4 + c_5(V_{s\text{-}30}) + c_6 + c_7(z_{1.5}) \tag{14}$$

where c_6 and c_7 are coefficients determined by regression analysis. Note that the site term for basin effects is additive, as was the $V_{s\text{-}30}$ term. Because only a relatively small subset of the database has depth parameters, regression analyses are performed with fixed values of c_4, c_5, source/distance parameters, and event terms from the base model. We utilize the regression equation:

$$\ln(SD)_{ij} = \ln[(SD_m)_{ij} + c_6 + c_7(z_{1.5})_{ij}] + \eta_i + \varepsilon_{ij} \tag{15}$$

where $(SD_m)_{ij}$ refers to the median prediction of the base model (Equation 13) for site j in event i (i.e., the term in brackets on the right-hand side of Equation 13), η_i is the event term for earthquake i, and ε_{ij} is the residual term defined previously. To define a regression equation in arithmetic units, we set ε_{ij}=0 and take the exponent of both sides to obtain

$$(SD)_{ij}\varepsilon^{-\eta} - (SD_m)_{ij} = c_6 + c_7(z_{1.5})_{ij} \tag{16}$$

Regressions to estimate c_6 and c_7 were least squares, which gives equal weight to each data point. This is appropriate because of the inclusion of the event term in Equation 16.

One set of regression analyses utilizes all data for which $z_{1.5}$ is defined. Results are given in Table 7 in rows labeled "All," and example plots of residuals against $z_{1.5}$ are given in Figure 11a. Significant-duration parameters other than $D_{a5\text{-}75}$ have statistically significant depth dependence, as seen by the relatively high rejection confidence (1-p) values for the zero slope null hypothesis. Parameter $D_{a5\text{-}75}$ tends to be more dominated by body waves than the other duration parameters considered, and the duration of body waves would not be expected to be significantly affected by basin geometry. This may explain the lack of depth dependence for $D_{a5\text{-}75}$. Surface waves can significantly contribute to the other duration parameters, so the depth dependence observed for those parameters is not surprising. The size of the correction for those parameters ranges from nearly zero at shallow depth to 3–4 s at about 3,500 m depth.

Additional regression analyses were performed for deep basin sites ($z_{1.5}$ > 500 m) with the data segregated according to whether the source underlies the basin (coincident source and site basin locations, denoted as CBL) or is located outside of the basin perimeter (distinct source and site basin locations, denoted as DBL). These results are also given in Table 7, with representative plots in Figures 11b and 11c. CBL consistently shows stronger depth dependence than DBL. The CBL depth dependence is towards decreasing duration in deeper basins, whereas DBL shows the opposite. Durations for DBL

Table 7. Regression coefficient showing dependence of base model residuals on basin parameters

	Group	c_6 (s)	c_7 (s/m)	Std Dev. (s)	$1-p^*$
$D_{a5\text{-}75}$	All	0.40±0.22	3.0E−05±1.9E−04	3.41	0.13
	CBL	1.91±0.75	−7.5E−04±4.2E−04	2.86	0.93
	DBL	−0.08±0.62	7.0E−04±4.3E−04	4.21	0.89
$D_{a5\text{-}95}$	All	−0.44±0.44	1.2E−03±3.7E−04	6.73	1.00
	CBL	3.25±1.17	−1.2E−03±6.5E−04	4.44	0.94
	DBL	0.09±1.25	9.3E−04±8.6E−04	8.41	0.72
$D_{v5\text{-}75}$	All	−0.26±0.37	1.1E−03±3.1E−04	5.60	1.00
	CBL	4.43±1.05	−1.9E−03±5.8E−04	4.01	1.00
	DBL	0.43±1.00	7.8E−04±6.9E−04	6.74	0.74
$D_{v5\text{-}95}$	All	−0.14±0.55	7.7E−04±4.7E−04	8.47	0.90
	CBL	5.52±1.31	−2.7E−03±7.3E−04	4.97	1.00
	DBL	0.78±1.60	2.5E−04±1.1E−03	10.79	0.18

* rejection confidence for a $c_7=0$ model (null hypothesis of zero slope)

consistently exceed those for CBL at $z_{1.5} > \sim 1500$ m. The larger durations for the DBL case are expected because basin edge effects can generate surface waves that travel across the basin (Graves 1993). The CBL case is dominated by body waves entering the sediments from beneath; we speculate that durations may decrease with depth because of increasing effects of material damping, which can reduce high-frequency motions at the beginning of records to the extent that they do not contribute to significant duration. Despite the physically meaningful differences between the data trends for CBL and DBL, the scatter of the limited available data is such that the statistical distinction between the two data sets is only marginally significant per the F-test (Cook and Weiberg 1999).

Given the marginal CBL/DBL distinction, the preferred approach for most applications is to use the coefficients labeled "All" in Table 7 when correcting for basin effects with Equation 14, although no depth correction is needed for $D_{a5\text{-}75}$. The general magnitude of the basin corrections can be as large as the corrections for shallow site conditions (up to 3–4 s in both cases). Both site effects should be considered in the prediction of significant duration for engineering design.

DEPENDENCE OF BASE MODEL RESIDUALS ON NEAR-FAULT PARAMETERS

Somerville et al. (1997) found that near-fault forward directivity effects reduce strong-motion duration. Their model for rupture directivity modifies the Abrahamson and Silva (1996) model, which does not consider near-fault effects.

We evaluate near-fault effects on significant duration using residuals defined as follows:

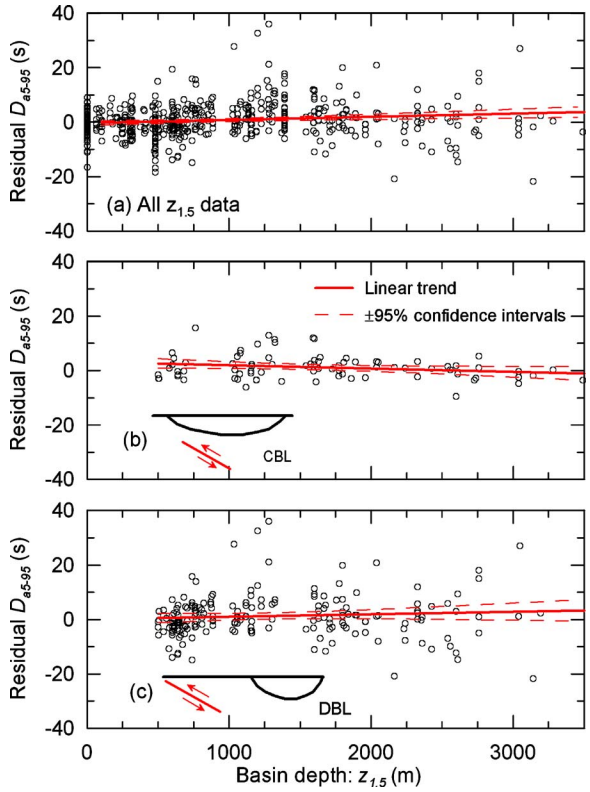

Figure 11. Residuals of base model for $D_{a5\text{-}95}$ with respect to basin depth for (a) overall database, (b) sites with coincident source and site basin locations (CBL), and (c) sites with distinct source and site basin locations (DBL). Residuals are defined per left-hand side of Equation 16.

$$\varepsilon_{ij} = \ln(SD)_{ij} - [\ln(SD_m)_{ij} + \eta_i] \tag{17}$$

where ε_{ij}=residual for recording j in event i (same as residual term used in Equation 13), η_i=event term for event i, SD_{ij}=significant duration calculated from recording j, and $(SD_m)_{ij}$=significant duration calculated from the base regression model (Equation 13) with $\varepsilon_{ij}=0$.

Regression analyses were performed to relate residuals as defined from Equation 17 to rupture directivity parameters and to distance for $M>6$ earthquakes and site-source distances $r<20$ km. The distance cutoff of 20 km was selected because of the bias at $r<20$ km in the base model (Figure 8). The magnitude cutoff of 6.0 was selected based on previous experience (Somerville et al. 1997, Liu et al. 2001). Regressions against rupture directivity parameters were performed using the equation

$$\varepsilon_{ij} = c_8 + c_9 RDP_{ij} + \kappa_{ij} \tag{18}$$

where c_8 and c_9 are regression coefficients, κ_{ij} is a residual term with zero mean and standard deviation σ, and RD_{ij} is a rupture directivity parameter that describes the degree to which the site is subject to forward versus backward directivity ($RDP > \sim 0.5$ for forward directivity, smaller values indicate backward or no directivity [Somerville et al. 1997]). Our results, which are presented in full in Kempton (2004), indicate statistically significant values of c_8 but not c_9. This indicates that near-fault effects are significant, but they do not correlate strongly with *RDP*. Accordingly, a second set of regression analyses were performed to relate residuals to distance:

$$\varepsilon_{ij} = c_{10}(r - 20) + \kappa_{ij} : r < 20 \text{ km}$$

$$\varepsilon_{ij} = 0 : r > 20 \text{ km} \tag{19}$$

where r=site-source distance in km, and c_{10} is a regression coefficient. Both Equations 18 and 19 provide additive corrections (in log units) to base Equation 13; hence they are multiplicative in arithmetic units. This is appropriate because near-fault forward directivity compresses the body wave field (the correction would be expected to be less applicable to surface waves). Regressions using Equations 18 and 19 are least squares, which gives equal weight to each data point. This is appropriate because of the inclusion of the event term in Equation 17.

Results obtained using Equation 19 are summarized in Table 8. Example plots of residuals versus distance are given in Figure 12. Positive values of c_{10} indicate decreased duration (relative to the base model) in near-fault regions. When interpreting these results, it is useful to begin with parameter $D_{a5\text{-}75}$, which tends to be more dominated by body waves than the other parameters considered. A body wave–dominated duration parameter would be expected to exhibit the clearest trends with respect to near-fault conditions because the wave stacking phenomena associated with rupture directivity occurs in shear waves and not surface waves. Moreover, near-fault effects tend to be stronger for strike-slip earthquakes than for dip-slip earthquakes (Somerville et al. 1997), and hence we initially focus on data for strike-slip earthquakes.

Figure 12 shows the residuals of data from strike-slip earthquakes against the base model along with the results of regression analyses for this data using Equation 19. Confidence intervals (±95%) are also shown around the fit line. The base model for $D_{a5\text{-}75}$ has no significant near-fault bias for backward directivity conditions in strike-slip earthquakes (i.e., c_{10} values are nearly zero) but a strong bias exists for forward-directivity conditions in strike-slip earthquakes (i.e., c_{10} values are positive and significantly nonzero). This is consistent with previous findings (Somerville et al. 1997) and expected patterns of behavior for shear waves.

As shown in Table 8, c_{10} values for the $D_{a5\text{-}75}$ parameter and dip-slip earthquakes are significantly positive but not significantly different for forward- and backward-directivity conditions. This suggests that some bias exists in the model formulation in near-fault regions that can be corrected by Equation 19, but this bias is unlikely to be

Table 8. Regression coefficients showing dependence of base model residuals on near-fault rupture directivity

	Slip type[1]	Directivity[2]	c_{10}	σ	p
$D_{a5\text{-}75}$	SS	Backward	0.007±0.005	0.373	0.166
		Forward	0.016±0.007	0.453	0.041
	DS	Backward	0.022±0.007	0.290	0.002
		Forward	0.016±0.010	0.480	0.133
	SS+DS	Backward	0.010±0.004	0.342	0.008
		Forward	0.016±0.006	0.149	0.010
$D_{a5\text{-}95}$	SS	Backward	0.014±0.004	0.337	0.003
		Forward	0.013±0.006	0.372	0.040
	DS	Backward	0.018±0.006	0.243	0.004
		Forward	0.015±0.007	0.353	0.056
	SS+DS	Backward	0.015±0.003	0.296	0.000
		Forward	0.014±0.005	0.361	0.004
$D_{v5\text{-}75}$	SS	Backward	0.020±0.006	0.446	0.001
		Forward	0.023±0.009	0.554	0.019
	DS	Backward	0.030±0.010	0.449	0.007
		Forward	0.023±0.012	0.616	0.083
	SS+DS	Backward	0.023±0.005	0.446	0.000
		Forward	0.023±0.007	0.569	0.003
$D_{v5\text{-}95}$	SS	Backward	0.020±0.005	0.360	0.000
		Forward	0.016±0.007	0.420	0.024
	DS	Backward	0.012±0.006	0.260	0.052
		Forward	0.026±0.009	0.464	0.014
	SS+DS	Backward	0.018±0.004	0.318	0.000
		Forward	0.020±0.006	0.434	0.001

[1] Oblique earthquakes are treated as SS or DS depending on orientation of principal rupture slip
[2] RDP $> \sim 0.5$ for forward directivity and RDP $< \sim 0.5$ for backward directivity

related to rupture directivity. We speculate that the lack of a clear rupture directivity effect for $D_{a5\text{-}75}$ in dip-slip earthquakes results from relatively modest rupture directivity (e.g., Somerville et al. 1997).

As shown by the results in Table 8, the other duration parameters considered ($D_{a5\text{-}95}$, $D_{v5\text{-}75}$, and $D_{v5\text{-}95}$) show no significant differences between the results for strike-slip versus dip-slip earthquakes nor for forward versus backward directivity. We speculate that this lack of a clear rupture directivity effect occurs because these duration parameters are sensitive to surface waves, which are not subject to rupture directivity effects.

Based on these results, we recommend that the base model be corrected for near-fault conditions using Equation 19 with the c_{10} coefficients given in Table 9. This cor-

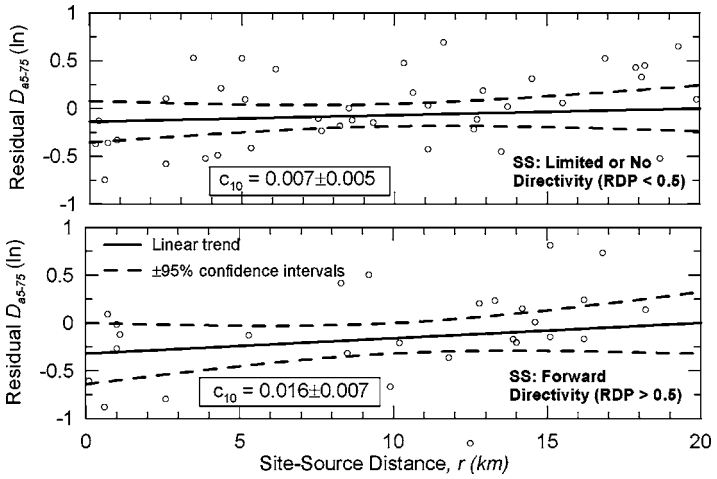

Figure 12. Residuals of base model for $D_{a5\text{-}75}$ with respect to site-source distance for case of limited or no directivity (top frame) and forward directivity (bottom frame). Data shown are from strike-slip earthquakes.

rects for rupture directivity effects when applied to parameter $D_{a5\text{-}75}$ and strike-slip earthquakes; otherwise it simply corrects for bias in the distance term used in the base model. The intra-event standard-deviation terms (σ) given in Table 8 are similar to those for the base model (Table 6); hence no adjustments to dispersion terms are needed when using the near-fault corrections. The effects of these near-fault corrections on the $D_{a5\text{-}75}$ and $D_{a5\text{-}95}$ median predictions are shown in Figure 13.

COMPARISONS TO PREVIOUS STUDIES

Figures 14 and 15 compare significant durations from our base model (with near-fault corrections) to predictions from previous models. Figure 14 illustrates magnitude scaling for r=30 km and rock sites. The trend of our results is similar to that of Trifunac and Brady (1975), Kamiyama (1984), and Abrahamson and Silva (1996). The slopes of the duration-magnitude curves increase with magnitude in our model, an effect shown previously only by Abrahamson and Silva (1996).

Table 9. Recommended values of parameter c_{10}

	$D_{a5\text{-}75}$		$D_{a5\text{-}95}$	$D_{v5\text{-}75}$	$D_{v5\text{-}95}$
	SS	DS	SS+DS	SS+DS	SS+DS
C_{10}	0 (bkwd) 0.016 (frwd)	0.020	0.015	0.023	0.019

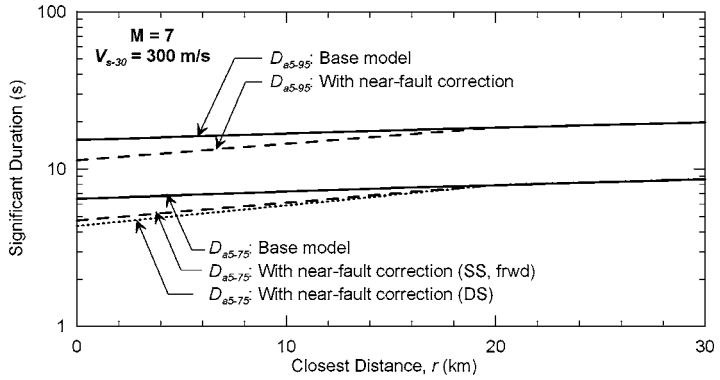

Figure 13. Median durations ($D_{a5\text{-}75}$ and $D_{a5\text{-}95}$) for base models and base models with near-fault corrections for M=7 earthquake at soil site with $V_{s\text{-}30}$=300 m/s. Note that there is no correction for strike-slip faulting with backward directivity (SS, bkwd).

The distance scaling shown in Figure 15 indicates a similar trend on rock for our results and those of Trifunac and Brady (1975) and Abrahamson and Silva (1996). That trend consists of negligible distance dependence at close distance ($r < \sim 20$ km) and increasing slope as r increases. Other models tend to show relatively flat slopes (Dobry et al. 1978, Kamiyama 1984) or distance invariant slopes on a log scale (McGuire and Barnhard 1979). These differences result from the use of a distance term that is additive to the source duration (Trifunac and Brady 1975, Abrahamson and Silva 1996, this study) versus one that is multiplicative (Dobry et al. 1978, McGuire and Barnhard 1979, Kamiyama 1984).

We found significant duration to increase with decreasing $V_{s\text{-}30}$. Shown in Figure 16 is the $V_{s\text{-}30}$-based site term from this study relative to similarly formatted (i.e., additive)

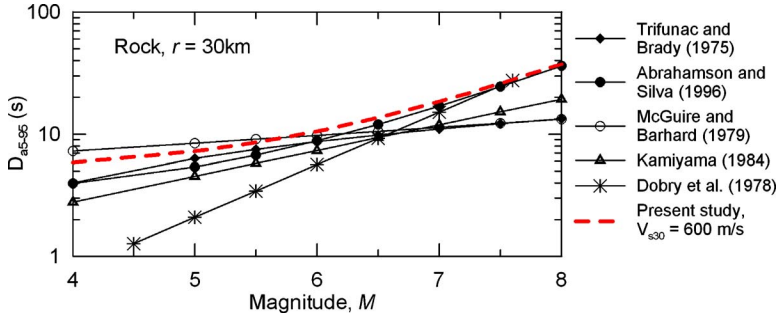

Figure 14. Comparison of magnitude dependence of base model from this study with results of previous research for rock sites.

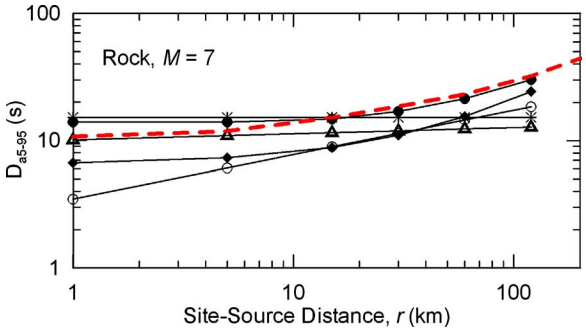

Figure 15. Comparison of distance dependence of base model from this study with results of previous research for rock sites (see legend in Figure 14).

site terms from previous investigators (Trifunac and Brady 1975, Abrahamson and Silva 1996). The site terms are similar in the sense that larger significant durations are consistently found on soil than on rock. However, the magnitude of the duration change with site condition (as measured by the "slope" of the relations) is different among the three studies, with our factors having a slope intermediate between those of Trifunac/Brady and Abrahamson/Silva. Other investigators used a multiplicative site term that cannot be readily compared to those shown in Figure 16 (McGuire and Barnhard 1979, Kamiyama 1984). No previous investigators have developed additive site terms for basin effects on significant duration, so no comparisons are possible.

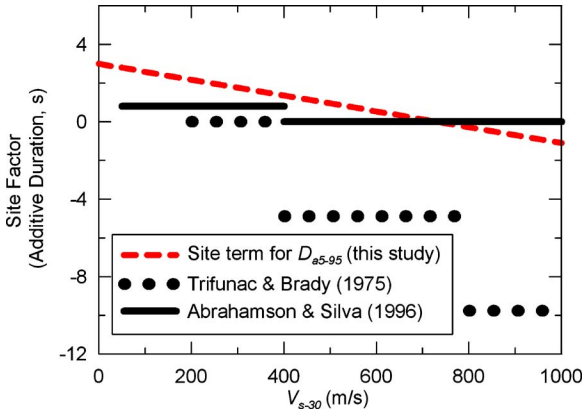

Figure 16. Comparison of additive site term from this study with similar site terms from previous research. Abrahamson and Silva (1996) site categories are soil and rock. Trifunac and Brady site categories are soft alluvium, intermediate rock, and hard rock. The velocity ranges indicated are our estimates of the range of conditions that would be present for each category.

SUMMARY AND CONCLUSIONS

We have developed prediction equations for the significant duration of earthquake ground motion as a function of magnitude, closest site-source distance, near-surface shear-wave velocity ($V_{s\text{-}30}$), basin depth, and near-fault parameters. The model was developed using a worldwide strong-motion database of recordings from active tectonic regions such as California and portions of Japan, Turkey, and Taiwan.

Significant duration is found to increase strongly with earthquake magnitude and moderately with distance. The model is considered valid across a magnitude range of $M \approx 5$ to 7.6 and a distance range of $r \approx 0$ to 200 km. The base model represented by Equation 13 and Table 6 includes a site term that is dependent on the near-surface shear-wave velocity ($V_{s\text{-}30}$). A statistically significant dependence of duration on $V_{s\text{-}30}$ was found, with duration increasing as velocity decreases. Residuals of the base model are correlated with basin depth for significant-duration parameters other than $D_{a5\text{-}75}$. Duration tends to decrease with depth when the seismic source is located beneath the basin, and increase with depth when the source and basin locations are distinct. For current application, however, a simple model that does not consider source location is likely adequate (Equation 14 with coefficients in Table 7 from rows labeled "All").

The near-fault correction is an important part of the model because of overprediction bias for $M > 6$ and $r < 20$ recordings. For parameter $D_{a5\text{-}75}$, distance-dependent near-fault factors reduce that bias when applied to strike-slip earthquakes and sites subject to forward directivity. Near-fault corrections for other duration parameters are apparently unrelated to rupture directivity effects, but the corrections are nonetheless significant. The near-fault correction to the base model is presented in Equation 19 with coefficients in Table 9.

The total standard deviation of the duration models varies from a minimum of 0.44 (for $D_{a5\text{-}95}$) to a maximum of 0.68 (for $D_{v5\text{-}75}$) in natural logarithmic units. These standard-deviation terms are comparable to what is generally obtained for response spectral acceleration. The standard-deviation terms have contributions from both intra- and inter-event variability in the data. The intra-event variability is the larger of the two, being about 20–40% larger than inter-event variability. Dispersion terms are not significantly affected by the near-fault corrections, although significant reductions in standard deviation were achieved by refining the source and site functions in the development of the base model.

ACKNOWLEDGMENTS

The work presented in this paper benefited from support provided by the Pacific Earthquake Engineering Research Center through the Earthquake Engineering Research Centers Program of the National Science Foundation under Award Number EEC-9701568. Any opinions, findings, and conclusions or recommendations expressed in this material are those of the authors and do not necessarily reflect those of the National Science Foundation. Drs. Yoojoong Choi and Rick Schoenberg are thanked for their assistance with the statistical analyses. Dr. Julian Bommer and two anonymous reviewers are thanked for their comments, which improved the manuscript.

REFERENCES

Abrahamson, N. A., and Silva, W. J., 1996. Empirical Ground Motion Models, Report to Brookhaven National Laboratory.

Abrahamson, N. A., and Youngs, R. R., 1992. A stable algorithm for regression analyses using the random effects model, *Bull. Seismol. Soc. Am.* **82**, 505–510.

Anderson, J. G., 2004. Quantitative measure of goodness-of-fit of synthetic seismographs, *Proceedings, 13th World Conference on Earthquake Engineering, Vancouver, B.C., Canada*, Paper 243.

Ang, A. H.-S., and Tang, W. H., 1975. *Probability Concepts in Engineering Planning and Design, Volume I—Basic Principles*, John Wiley & Sons, New York.

Arias, A., 1970. A measure of earthquake intensity, in *Seismic Design for Nuclear Power Plants*, edited by R. Hansen, MIT Press, Cambridge, MA, pp. 438–483.

Atkinson, G. M., and Beresnev, I. A., 1997. Don't call it stress drop, *Seismol. Res. Lett.* **68**, 3–4.

Bolt, B. A., 1973. Duration of strong ground motions, *Proceedings, 5th World Conference on Earthquake Engineering, Acapulco*, Paper 84.

Bommer, J. J., and Martinez-Pereira, A., 1999. The effective duration of earthquake strong motion, *J. Earthquake Eng.* **3**, 127–172.

Bommer, J. J., Magenes, G., Hancock, J., and Penazzo, P., 2004. The influence of strong motion duration on the seismic response of masonry structures, *Bull. Earthquake Eng.* **2** (1), 1–26.

Bommer, J. J., Hancock, J., and Alarcón, J. E., 2006. Correlations between duration and number of effective cycles of earthquake ground motion, *Soil Dyn. Earthquake Eng.* **26** (1), 1–13.

Boore, D. M., 1983. Stochastic simulation of high-frequency ground motions based on seismological models of the radiated spectra, *Bull. Seismol. Soc. Am.* **73**, 1865–1894.

———, 2001, Comparisons of ground motions from the 1999 Chi-Chi earthquake with empirical predictions largely based on data from California, *Bull. Seismol. Soc. Am.* **91**, 1212–1217.

Borcherdt, R. D., 1994. Estimates of site-dependent response spectra for design (methodology and justification), *Earthquake Spectra* **10** (4), 617–653.

———, 2002, Empirical evidence for acceleration-dependent amplification factors, *Bull. Seismol. Soc. Am.* **92**, 761–782.

Borcherdt, R. D., and Glassmoyer, G., 1994. Influences of local geology on strong and weak ground motions recorded in the San Francisco Bay region and their implications for site-specific building-code provisions, *The Loma Prieta, California Earthquake of October 17, 1989—Strong Ground Motion, U.S. Geol. Surv. Prof. Pap. 1551-A*, A77–A108.

Chai, Y. H., Fajfar, P., and Romstad, K. M., 1998. Formulation of duration-dependent inelastic seismic design spectrum, *J. Struct. Eng.* **124**, 913–921.

Choi, Y., and Stewart, J. P., 2005. Nonlinear site amplification as function of 30 m shear wave velocity, *Earthquake Spectra* **21** (1), 1–30.

Choi, Y., Stewart, J. P., and Graves, R. W., 2005. Empirical model for basin effects that accounts for basin depth and source location, *Bull. Seismol. Soc. Am.* **95**, 1412–1427.

Cook, R. D., and Weiberg, S., 1999. *Applied Regression Including Computing and Graphics*, John Wiley & Sons, New York.

Cornell, C. A., 1997. Does duration really matter? *Proceedings of the FHWA/NCEER Workshop on the National Representation of Seismic Ground Motion for New and Existing Highway Facilities*, pp. 125–133.

Dobry, R., Idriss, I. M., and Ng, E., 1978. Duration characteristics of horizontal components of strong-motion earthquake records, *Bull. Seismol. Soc. Am.* **68**, 1487–1520.

Dobry, R., Borcherdt, R. D., Crouse, C. B., Idriss, I. M., Joyner, W. B., Martin, G. R., Power, M. S., Rinne, E. E., and Seed, R. B., 2000. New site coefficients and site classification system used in recent building seismic code provisions, *Earthquake Spectra* **16** (1), 41–67.

Graves, R. W., 1993. Modeling three-dimensional site response effects in the Marina District, San Francisco, California, *Bull. Seismol. Soc. Am.* **83**, 1042–1063.

Hancock, J., and Bommer, J. J., 2004. The influence of phase and duration on earthquake damage in degrading structures, *Proceedings, 13th World Conference on Earthquake Engineering, Vancouver, B.C., Canada*, Paper 1990.

———, 2005. The effective number of cycles of earthquake ground motion, *Earthquake Eng. Struct. Dyn.* **34**, 637–664.

Hanks, T. C., and Kanamori, H., 1979. A moment magnitude scale, *J. Geophys. Res.* **84**, 2348–2350.

Hanks, T. C., and McGuire, R. K., 1981. The character of high frequency strong ground motion, *Bull. Seismol. Soc. Am.* **71**, 2071–2095.

Hole, J. A., Brocher, T. M., Klemperer, S. L., Parsons, T., Benz, H. M., and Furlong, K. P., 2000. Three-dimensional seismic velocity structure of the San Francisco Bay area, *J. Geophys. Res.* **105** (B6), 13859–13874.

Husid, L. R., 1969. Características de terremotos, Análisis general, Revista del IDIEM 8, Santiago del Chile, pp. 21–42.

Iervolino, I., Manfredi, G., and Cosenza, E., 2006. Ground motion duration effects on nonlinear seismic response, *Earthquake Eng. Struct. Dyn.* **35** (1), 21–38.

Kamiyama, M., 1984. Effects of subsoil conditions and other factors on the duration of earthquake ground shaking, *Proceedings, 8th World Conference on Earthquake Engineering, San Francisco*, Vol. 2, pp. 793–800.

Kempton, J. J., 2004. Prediction Models for Significant Duration of Earthquake Ground Motions, M.S. dissertation, University of California, Los Angeles.

Liu, A. H., Stewart, J. P., Abrahamson, N. A., and Moriwaki, Y., 2001. Equivalent number of uniform stress cycles for soil liquefaction analyses, *J. Geotech. Geoenviron. Eng.* **127**, 1017–1026.

Magistrale, H., Day, S., Clayton, R., and Graves, R., 2000. The SCEC southern California reference three-dimensional seismic velocity model version 2, *Bull. Seismol. Soc. Am.* **90**, S65–S76.

McGuire, R. K., and Barnhard, T. P., 1979. The usefulness of ground motion duration in prediction of severity of seismic shaking, *Proceedings, 2nd U.S. National Conference on Earthquake Engineering, Stanford, Calif.*, pp. 713–722.

Mohraz, B., and Peng, M.-H., 1989. The use of low-pass filtering in determining the duration of strong ground motion, *Publication PVP-182*, Pressure Vessels and Piping Division, ASME, pp. 197–200.

Novikova, E. I., and Trifunac, M. D., 1994. Duration of strong ground motion in terms of earthquake magnitude, epicentral distance, site conditions and site geometry, *Earthquake Eng. Struct. Dyn.* **23**, 1023–1043.

Pinheiro, J. C., and Bates, D. M., 2000. *Mixed-Effects Models in S and S-PLUS*, Springer-Verlag, New York.

Rauch, A. F., and Martin, J. R., 2000. EPOLLS model for predicting average displacements on lateral spreads, *J. Geotech. Engrg.* **126**, 360–371.

Reinoso, E., Ordaz, M., and Guerrero, R., 2000. Influence of strong ground-motion duration in seismic design of structures, *Proceedings, 12th World Conference on Earthquake Engineering*, Paper 1151.

Sarma, S. K., 1970. Energy flux of strong earthquakes, *Tectonophysics* **11**, 159–173.

Seed, H. B., and Lee, K. L., 1966. Liquefaction of saturated sands during cyclic loading, *J. Soil Mech. and Found. Div.* **92**, 105–134.

Shome, N., Cornell, C. A., Bazzurro, P., and Carballo, J. E., 1998. Earthquakes, records, and nonlinear responses, *Earthquake Spectra* **14** (3), 469–500.

Silver, M. L., and Seed, H. B., 1971. Volume changes in sands during cyclic loading, *J. Soil Mech. and Found. Div.* **97**, 1171–1182

Somerville, P. G., Smith, N. F., Graves, R. W., and Abrahamson, N. A., 1997. Modification of empirical strong ground motion attenuation relations to include the amplitude and duration effects of rupture directivity, *Seismol. Res. Lett.* **68**, 199–222.

Stewart, J. P., Liu, A. H., Choi, Y., and Baturay, M. B., 2001. Amplification Factors for Spectral Acceleration in Active Regions, Report No. *PEER-2001/10*, Pacific Earthquake Engineering Research Center, University of California, Berkeley.

Stewart, J. P., Choi, Y., and Graves, R. W., 2005. Empirical Characterization of Site Conditions on Strong Ground Motion, Report No. *PEER-2005/01*, Pacific Earthquake Engineering Research Center, University of California, Berkeley.

Tiwari, A. K., and Gupta, V. K., 2000. Scaling of ductility and damage-based strength reduction factors for horizontal motions, *Earthquake Eng. Struct. Dyn.* **29** (7), 969–987.

Trifunac, M. D., and Brady, A. G., 1975. A study on duration of strong earthquake ground motion, *Bull. Seismol. Soc. Am.* **65**, 581–626.

Trifunac, M. D., and Westermo, B. D., 1977. A note on the correlation of frequency-dependent duration of strong earthquake ground motion with the modified Mercalli intensity and the geologic conditions at the recording site, *Bull. Seismol. Soc. Am.* **67**, 917–927.

Vanmarcke, E. H., and Lai, S.-S. P., 1980. Strong motion duration and RMS amplitude of earthquake records, *Bull. Seismol. Soc. Am.* **70**, 1293–1307.

(Received 18 August 2005; accepted 22 December 2005)